

Non-conservative Rayleigh scattering in a finite atmosphere—I. Polarization of skylight

K. E. Rangarajan¹, D. Mohan Rao¹ and K. D. Abhyankar²

¹Indian Institute of Astrophysics, Bangalore 560 034

²Astronomy Department, Osmania University, Hyderabad 500 007

Received 1994 February 18; accepted 1994 March 29

Abstract. Non-conservative Rayleigh scattering in finite atmospheres is studied for various values of ω , where ω is the albedo for single scattering. The atmosphere is stratified into plane-parallel homogeneous layers. The sky polarization is plotted for certain typical positions of the sun.

We find that for the transmitted light the Babinet and Brewster neutral points in the principal meridian are brought closer to the sun for the lesser value of ω , while the Arago neutral point moves towards the anti-solar point with decreasing ω . As the albedo ω decreases, we get higher amount of polarization in the region where $I_l < I_r$ but lower amount of polarization where $I_l > I_r$. Here I_l and I_r refer to the components of intensity in two perpendicular directions. The increase in total optical thickness of the medium does not alter the amount of polarization for lower ω , but for higher ω , the amount of polarization is reduced for higher optical thickness. The reflected light behaves similar to the transmitted light for all the azimuthal directions of the sun. If the sun is not near the horizon, neutral points are seen in the principal meridian for all optical thickness.

Key words : polarization—earth's atmosphere—radiative transfer

1. Introduction

1.1. Conservative Rayleigh scattering

The main mechanisms for producing polarization in the earth's atmosphere are Rayleigh scattering by the gaseous molecules and other aerosol particles of various sizes which exhibit Mie scattering. The problem of conservative scattering according to Rayleigh's law in planetary atmospheres and the resulting polarization was formulated and solved by Chandrasekhar (1960). He considered both finite and semi-infinite atmospheres. He could explain the occurrence of the neutral polarization points of Arago, Babinet and Brewster. Using his method, Coulson, Dave & Sekera (1960) calculated all the three Stokes' parameters (I , Q , U) of the linearly polarized radiation in transmitted and reflected light for different positions of the sun in the

sky. Their extensive tables contain results for various optical depths and ground reflection coefficients.

1.2. *Non-conservative scattering—a realistic situation*

The radiation field incident on a gaseous medium is in general partly absorbed and partly scattered. Therefore the extinction of the radiation field consists of absorption and scattering. We can define the albedo for single scattering ω , as the ratio of scattering and extinction coefficients. i.e. $\omega = \sigma/(\sigma + k)$, where σ is the scattering coefficient and k the absorption coefficient. In a conservative scattering medium, $\omega = 1$. Since the radiation field undergoes absorption by small particles, we do find $\omega \neq 1$. This is referred to as non-conservative scattering.

1.2.1. SOME IMPORTANT OBSERVATIONAL RESULTS

Electronic polarimeters have been used for skylight measurements beginning in the 1950s by many workers including Sekera *et al.* (1956), Holzworth & Rao (1965), Coulson (1971, 1973) and several others. Here we will pertain ourselves to the data taken under clear atmospheric conditions. The major discrepancies between these observational results and those expected in the conservative Rayleigh scattering case are '*a shift of Babinet and Brewster points toward the sun*'. This is one observational point which we could account for by non-conservative Rayleigh scattering in the present study. In general there is a decrease of polarization in both positive and negative areas of the field except in one observation (Coulson 1973) where there is an increase in positive and a decrease in negative area of polarization (between Babinet and Brewster points). We have made an attempt to see whether non-conservative scattering could explain these results.

1.2.2. THEORETICAL CALCULATIONS

Scalar radiative transfer equation for finite media with non-conservative Rayleigh scattering was first solved using matrix method by Plass *et al.* (1973). Later they extended this method and studied the effect of haze layers on polarization (Kattawar *et al.* 1976). They assumed the haze particles to scatter according to Mie scattering law and obtained a value of 0.7171 for the single scattering albedo. The problem of non-conservative (imperfect) Rayleigh scattering in semi-infinite atmospheres was solved by Abhyankar & Fymat (1970). They considered various albedos (ω 's) in the range (0, 1). They found out that small ω 's increase the percentage of polarization compared to the conservative scattering. The radiation field encounters finite optical thickness in most of the situations and hence the assumption of semi-infinite atmosphere has limited use. Therefore in this paper, we address the problem of non-conservative Rayleigh scattering in finite atmospheres and our emphasis will be earth's atmosphere and the sky polarization. We employ a parametric study so that the effect of this scattering process on polarization can be better understood. Ground reflection has not been included in the present study. In general ground reflection leads to depolarization of radiation. Anisotropic particles also contribute to depolarization. Two excellent volumes have been written by Van de Hulst (1980) on multiple light scattering giving extensive tables, formulae and references to earlier work. In the next section, we describe the basic equations involved and our method of solution. In section 3, we have described the results.

2. Equation of transfer and the method of solution

We assume that the earth's atmosphere is stratified in plane-parallel homogeneous layers along z -axis. We assume that a parallel beam of (unpolarised) solar radiation of net flux πF per unit normal itself is incident on the atmosphere in direction $-\mu_0, \phi_0$. Here μ_0 is the cosine of the angle made by the ray to z -axis and ϕ_0 is the azimuth referred to a suitable chosen x -axis. Specific intensity of parallel beam of radiation has an angular distribution which can be expressed in terms of Dirac's δ -function in the form

$$I_{\text{inc}} = \pi F \delta(\mu - \mu_0) \delta(\phi - \phi_0). \quad \dots (1)$$

Due to singular character of this radiation field, we divide it into the unscattered part $\pi F e^{-\tau/\mu_0}$ and the diffuse field part that has experienced at least one scattering. For non conservative Rayleigh scattering atmosphere, the equation of transfer for a polarized beam is,

$$\begin{aligned} \mu \frac{d\mathbf{I}(\tau, \mu, \phi)}{d\tau} = & \mathbf{I}(\tau, \mu, \phi) - \frac{\omega}{4\pi} \int_0^{2\pi} \int_{-1}^{+1} \mathbf{P}(\mu, \phi; \mu', \phi') \mathbf{I}(\tau, \mu', \phi') d\mu' d\phi' \\ & - \frac{\omega}{4} \mathbf{P}(\mu, \phi; -\mu_0, \phi_0) F e^{-\tau/\mu_0}. \end{aligned} \quad \dots (2)$$

Optical depth $d\tau$ is given by $d\tau = -(k + \sigma)dz$. As the V component of \mathbf{I} separates out, the phase matrix for Rayleigh scattering with (I_b, I_r, U) components can be written (Chandrasekhar 1960) as

$$\begin{aligned} \mathbf{P}(\mu, \phi; \mu', \phi') = & \mathbf{Q}[\mathbf{P}^{(0)}(\mu, \mu') + (1 - \mu^2)^{1/2} (1 - \mu'^2)^{1/2} \mathbf{P}^{(1)}(\mu, \phi; \mu', \phi') \\ & + \mathbf{P}^{(2)}(\mu, \phi; \mu', \phi')], \end{aligned} \quad \dots (3)$$

where

$$\begin{aligned} \mathbf{Q} = & \begin{pmatrix} 1 & 0 & 0 \\ 0 & 1 & 0 \\ 0 & 2 & 2 \end{pmatrix} \\ \mathbf{P}^{(0)}(\mu, \mu') = & \frac{3}{4} \begin{pmatrix} 2(1 - \mu^2)(1 - \mu'^2) + \mu^2 \mu'^2 & \mu^2 & 0 \\ \mu'^2 & 1 & 0 \\ 0 & 0 & 0 \end{pmatrix} \end{aligned} \quad \dots (4)$$

$$\mathbf{P}^{(1)}(\mu, \phi; \mu', \phi') = \frac{3}{4} \begin{pmatrix} 4\mu\mu' \cos(\phi' - \phi) & 0 & 2\mu \sin(\phi' - \phi) \\ 0 & 0 & 0 \\ -2\mu' \sin(\phi' - \phi) & 0 & \cos(\phi' - \phi) \end{pmatrix} \quad \dots (5)$$

$$\mathbf{P}^{(2)}(\mu, \phi; \mu', \phi') = \frac{3}{4} \begin{pmatrix} \mu^2 \mu'^2 \cos 2(\phi' - \phi) & -\mu^2 \cos 2(\phi' - \phi) & \mu^2 \mu' \sin 2(\phi' - \phi) \\ -\mu'^2 \cos 2(\phi' - \phi) & \cos 2(\phi' - \phi) & -\mu' \sin 2(\phi' - \phi) \\ -\mu \mu'^2 \sin 2(\phi' - \phi) & \mu \sin 2(\phi' - \phi) & \mu \mu' \cos 2(\phi' - \phi) \end{pmatrix} \dots (6)$$

Chandrasekhar (1960) has given an elegant procedure to reduce the transfer equation to a set of equations which can be solved easily. Since we have followed the same procedure, we shall describe his approach briefly.

Mimicking the character of the Rayleigh phase matrix, we write

$$\mathbf{I}(\tau, \mu, \phi) = \mathbf{I}^{(0)}(\tau, \mu) + (1 - \mu^2)^{1/2} (1 - \mu_0^2)^{1/2} \mathbf{I}^{(1)}(\tau, \mu, \phi) + \mathbf{I}^{(2)}(\tau, \mu, \phi)$$

where $\mathbf{I}^{(0)}$ is azimuth independent and $\mathbf{I}^{(1)}$ and $\mathbf{I}^{(2)}$ contain terms in $(\phi - \phi_0)$ of period 2π and π only. As \mathbf{I} contains the three Stokes parameters namely $(I, I_r, U)^T$, equation (2) can be split into the following three equations :

$$\begin{aligned} \mu \frac{d\mathbf{I}^{(0)}(\tau, \mu)}{d\tau} &= \mathbf{I}^{(0)}(\tau, \mu) - \frac{\omega}{2} \int_{-1}^{+1} \mathbf{P}^{(0)}(\mu, \mu') \mathbf{I}^{(0)}(\tau, \mu') d\mu' \\ &\quad - \frac{\omega}{4} \mathbf{P}^{(0)}(\mu, \mu') \mathbf{F} e^{-\tau/\mu_0} \end{aligned} \dots (7)$$

$$\begin{aligned} \mu \frac{d\mathbf{I}^{(1)}}{d\tau} &= \mathbf{I}^{(1)} - \frac{\omega \mathbf{Q}}{4\pi} \int_{-1}^{+1} \int_0^{2\pi} (1 - \mu'^2) \mathbf{P}^{(1)}(\mu, \phi; \mu', \phi') \mathbf{I}^{(1)}(\tau, \mu', \phi') d\mu' d\phi' \\ &\quad - \frac{\omega \mathbf{Q}}{4} \mathbf{P}^{(1)}(\mu, \phi; -\mu_0, \phi_0) \mathbf{F} e^{-\tau/\mu_0} \end{aligned} \dots (8)$$

and

$$\begin{aligned} \mu \frac{d\mathbf{I}^{(2)}}{d\tau} &= \mathbf{I}^{(2)} - \frac{\omega \mathbf{Q}}{4\pi} \int_{-1}^{+1} \int_0^{2\pi} \mathbf{P}^{(2)}(\mu, \phi; \mu', \phi') \mathbf{I}^{(2)}(\tau, \mu', \phi') d\mu' d\phi' \\ &\quad - \frac{\omega \mathbf{Q}}{4} \mathbf{P}^{(2)}(\mu, \phi; -\mu_0, \phi_0) \mathbf{F} e^{-\tau/\mu_0}. \end{aligned} \dots (9)$$

Equations (8) and (9) allow solutions of the form

$$\begin{aligned} \mathbf{I}^{(1)}(\tau, \mu, \phi) &= \frac{\mathbf{Q}}{4} \mathbf{P}^{(1)}(\mu, \phi; -\mu_0, \phi_0) \mathbf{F} \phi^{(1)}(\tau, \mu) \\ \mathbf{I}^{(2)}(\tau, \mu, \phi) &= \frac{\mathbf{Q}}{4} \mathbf{P}^{(2)}(\mu, \phi; -\mu_0, \phi_0) \mathbf{F} \phi^{(2)}(\tau, \mu) \end{aligned} \dots (10)$$

where $\phi^{(1)}$ and $\phi^{(2)}$ are scalars. Then equations (8) and (9) can be written as

$$\mu \frac{d\phi^{(1)}}{d\tau} = \phi^{(1)} - \frac{3\omega}{8} \int_{-1}^{+1} (1 - \mu'^2)(1 + 2\mu'^2)\phi^{(1)}(\tau, \mu')d\mu' - \omega e^{-\tau/\mu_0},$$

$$\mu \frac{d\phi^{(2)}}{d\tau} = \phi^{(2)} - \frac{3\omega}{16} \int_{-1}^{+1} (1 + \mu'^2)^2\phi^{(2)}(\tau, \mu')d\mu' - \omega e^{-\tau/\mu_0}. \quad \dots (11)$$

We solve the system of equations (7) and (11) by using the discrete space theory technique (Grant & Hunt 1969, Peraiah 1978). The angular (μ) integration is done using a five point Gaussian quadrature mesh. Solutions are obtained for various combinations of μ , μ_0 , $\phi - \phi_0$ and various values of τ .

We obtained very good agreement with the results of Coulson, Dave & Sekera (1960) for the conservative scattering finite atmosphere. The results for non-conservative Rayleigh scattering in semi-infinite atmosphere were checked with those of Abhyankar & Fymat (1970).

3. Results

We define σ , the measure of polarization as $\sigma = \sqrt{Q^2 + U^2}/I$, where $Q = I_l - I_r$. Note that we have followed Chandrasekhar's definition regarding Q . A number of other workers in this field (Coulson *et al.* 1960; Plass *et al.* 1973) consider $Q = I_r - I_l$. We have calculated I_l , I_r , σ and $\chi = \tan^{-1}(U/Q)$ for various combinations of μ , μ_0 , $\phi - \phi_0$. We have considered the total optical thickness of the medium τ to be 0.2, 0.5 and 2.0. The different values of ω chosen are 0.2, 0.5, 0.8 and 1.0 and those for μ_0 are 0.1, 0.5 and 0.8. Computations are made for azimuthal angular differences $\phi - \phi_0 = 0, \pi/2$ and π . Figures 1 to 12 show the values at $\omega = 0.2$ (dash-dot line), $\omega = 0.5$ (dashed line), $\omega = 0.8$ (dotted line) and $\omega = 1.0$ (continuous line). All the quantities are plotted against the angle of observation $\theta = \cos^{-1} \mu$. Each figure contains a title which gives the values of the optical thickness τ , and μ_0 . For $\phi - \phi_0 = 0, \pi$, the Rayleigh phase matrix gives $U = 0$ for an unpolarized incident light, and therefore we have plotted only I , Q and σ for these cases. For $\phi - \phi_0 = \pi/2$, χ is also plotted as a function of θ .

General features for transmitted intensities

We find the following features from the figures. (i) The total intensity peaks at some angle θ . This peaking is more pronounced for small τ and large ω 's. The change in ω does not affect the angle at which the intensity becomes maximum whereas the optical thickness does affect the angle at which the intensity peaks. This fact can be used to differentiate between the optical thickness and the albedo effects. Higher optical thickness reduces the intensity and shifts the peak in the intensity towards the zenith. For smaller ω 's we find the intensity to be reduced which may be due to the increase in absorption. For smaller ω 's, I and Q are angle independent.

(ii) As ω is increased, $|Q|$ also increases at any angle θ . The increase in ω increases the probability for scattering to occur instead of absorption. Since scattering gives rise to the difference in I_l and I_r , $|Q|$ increases as ω is increased. When the sun is near the horizon ($\mu_0 = 0.1$), for smaller τ 's, $I_l > I_r$ at certain angles and $I_r > I_l$ at other angles. (i.e. Q changes

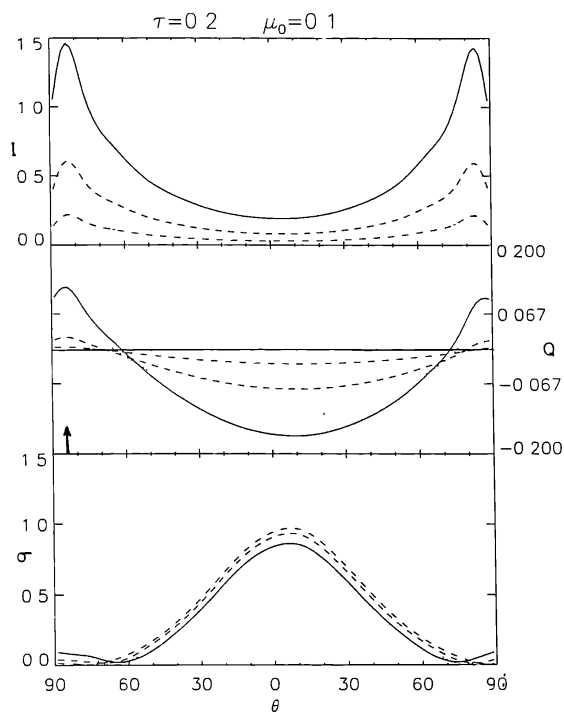


Figure 1(a). The abscissa represents the viewing zenith angle. The left side of $\theta = 0$ corresponds to the azimuth $\phi - \phi_0 = 0$ and the right side corresponds to the azimuth $\phi - \phi_0 = \pi$ i.e. solar and anti-solar directions. In the top panel we have the total transmitted intensity in terms of $\mu_0 F$, the middle panel shows Q and the lower most panel indicates σ in its ordinate. The total optical thickness (τ) and the sun's zenith angle ($\mu_0 = \cos(\theta_0)$) are shown as the heading of each figure. In all the figures, the solid line represents $\omega = 1.0$, the dotted line represents $\omega = 0.8$, the dash line shows the results for $\omega = 0.5$, and the dash-dot line indicates $\omega = 0.2$ results. The position of the sun is marked by an arrow.

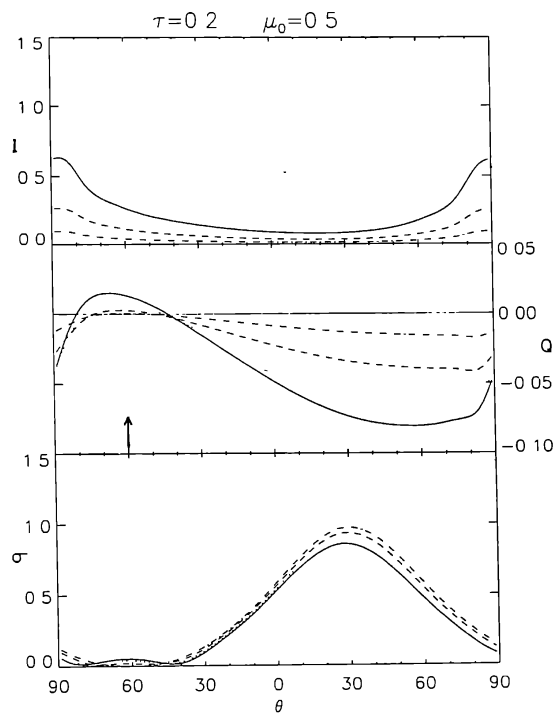


Figure 1(b). Same as figure 1(a) but for $\mu_0 = 0.5$.

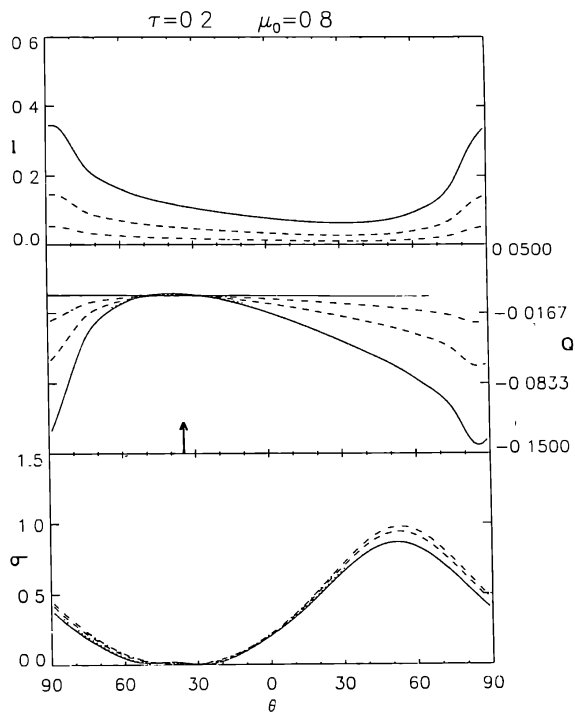


Figure 1(c). Same as figure 1(a) but for $\mu_0 = 0.8$

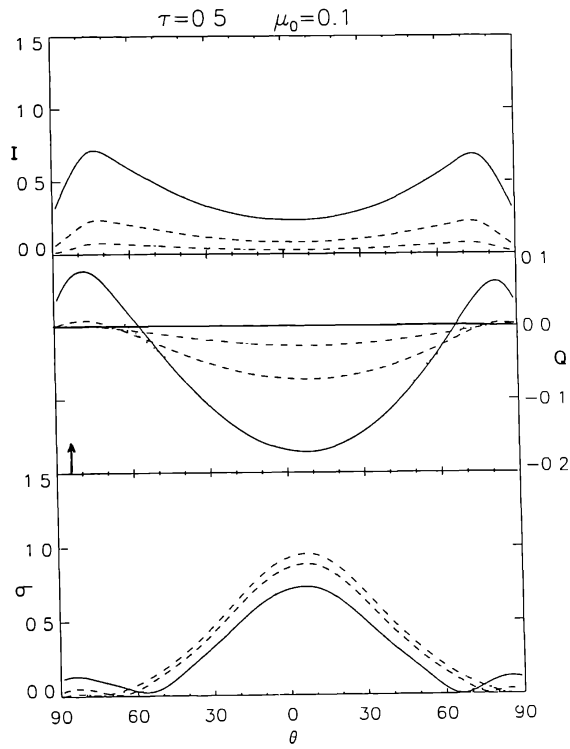


Figure 2(a). Same as figure 1(a) but for $\tau_0 = 0.5$

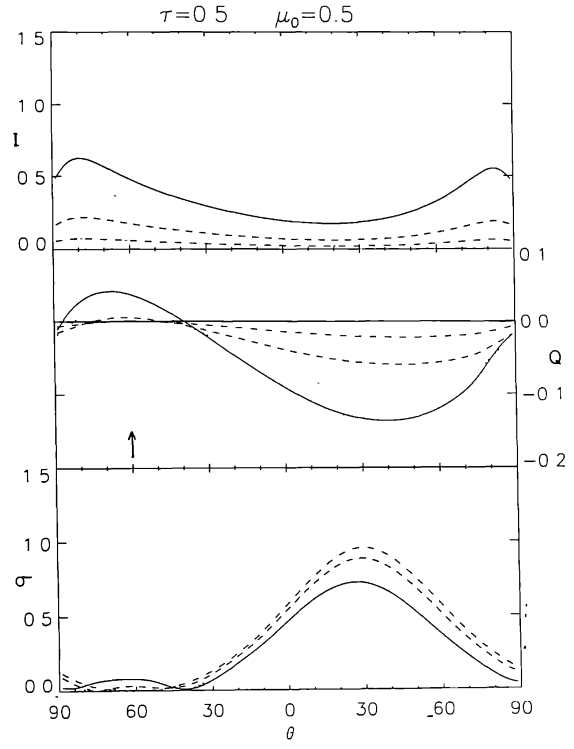


Figure 2(b). Same as figure 2(a) but for $\mu_0 = 0.5$.

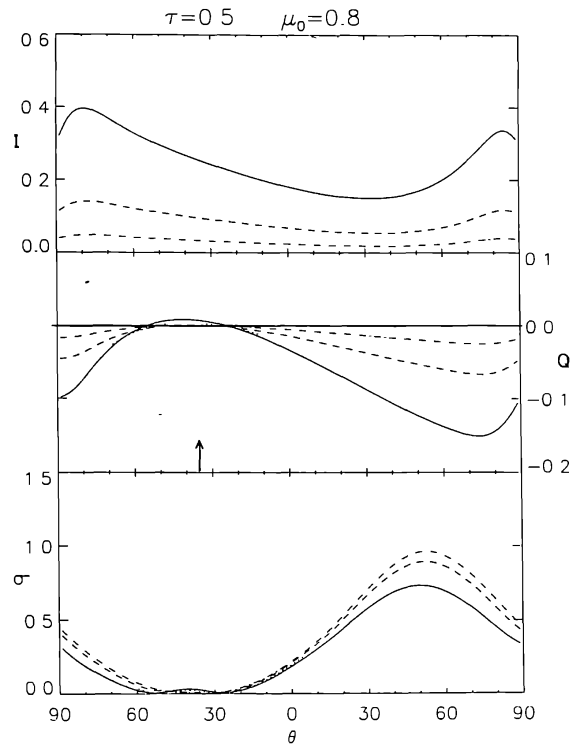
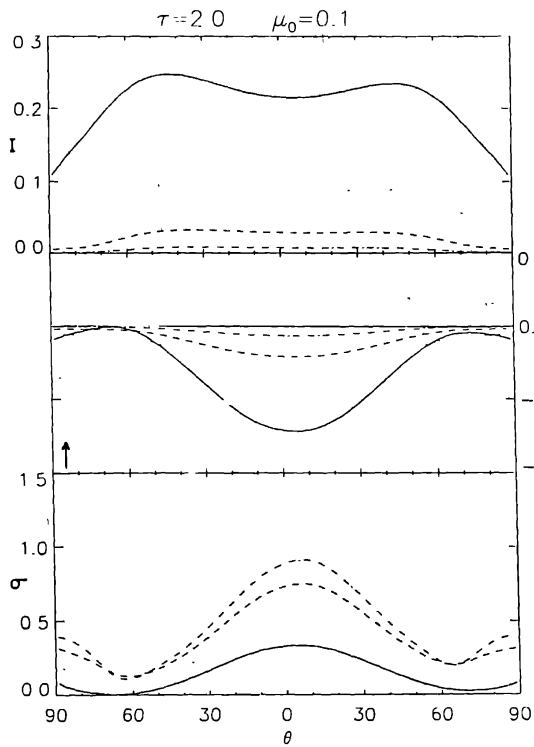
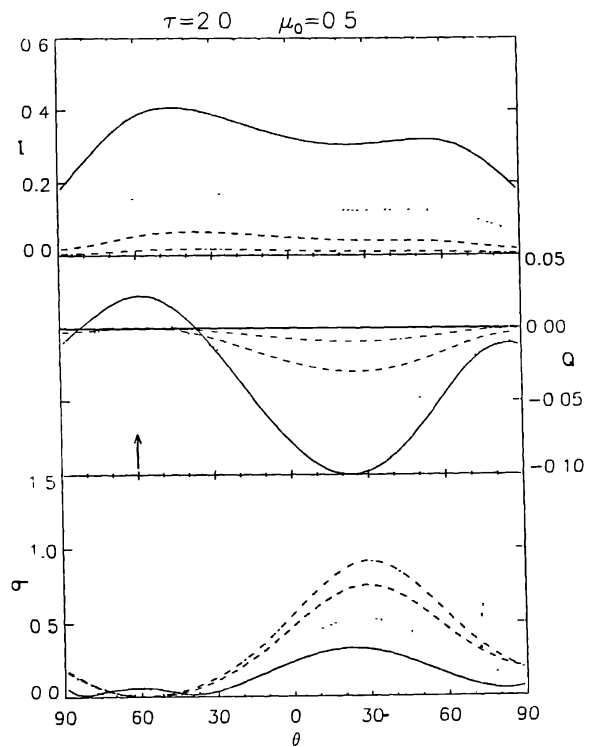
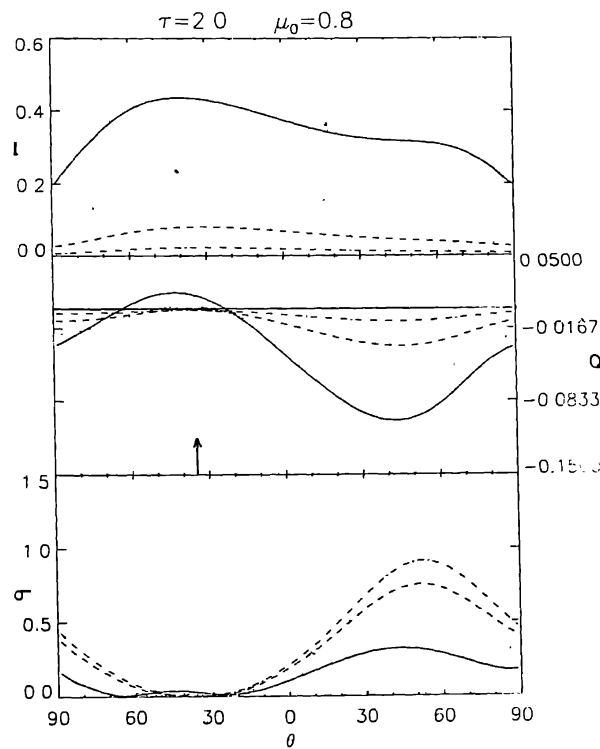


Figure 2(c). Same as figure 2(a) but for $\mu_0 = 0.8$.

Figure 3(a). Same as figure 1(a) but for $\tau = 2.0$.Figure 3(b). Same as figure 3(a) but for $\mu_0 = 0.5$.Figure 3(c). Same as figure 3(a) but for $\mu_0 = 0.8$.

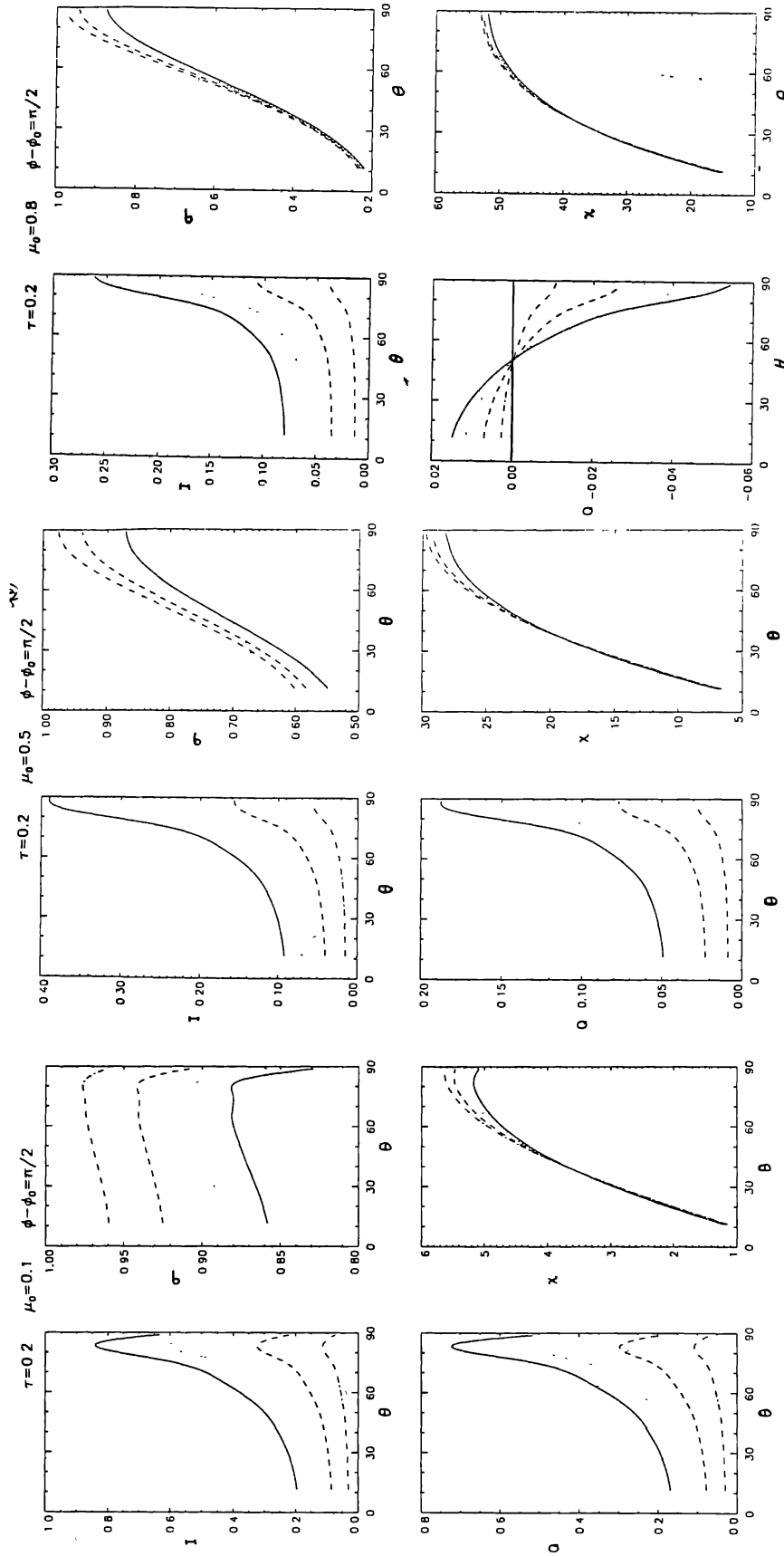


Figure 4(a). Top panels give total intensity (left) and Q (right) and the bottom panels show the Stokes V parameter and X at the azimuth angle $\phi - \phi_0 = \pi/2$ for $\tau = 0.2$ and $\mu_0 = 0.1$. Figure 4(b). Same as figure 4(a) but for $\mu_0 = 0.5$. Figure 4(c). Same as figure 4(a) but for $\mu_0 = 0.8$

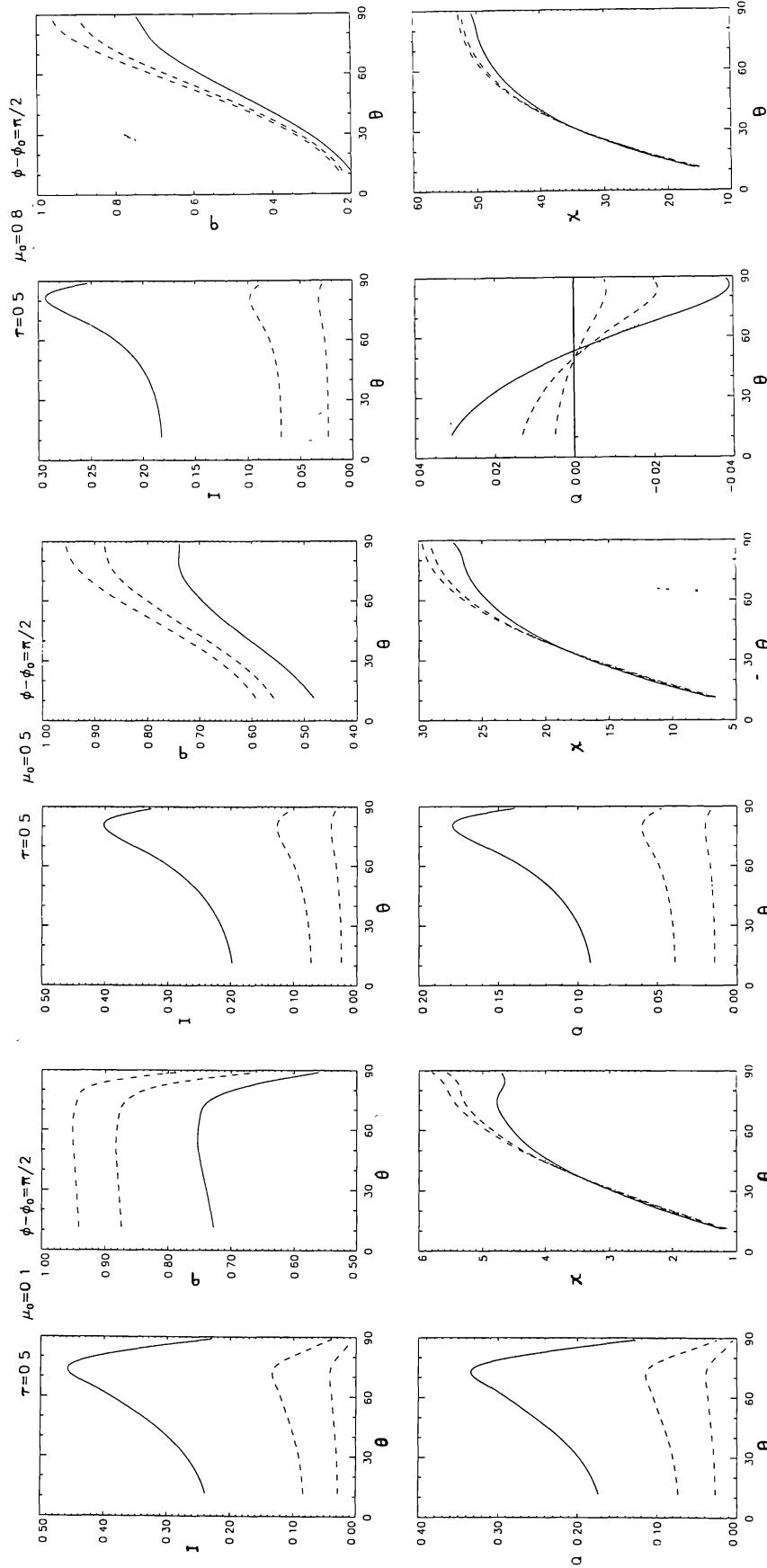


Figure 5(a). Same as figure 4(a) but for $\tau = 0.5$

Figure 5(b). Same as figure 5(a) but for $\mu_0 = 0.5$

Figure 5(c). Same as figure 5(a) but for $\mu_0 = 0.8$.

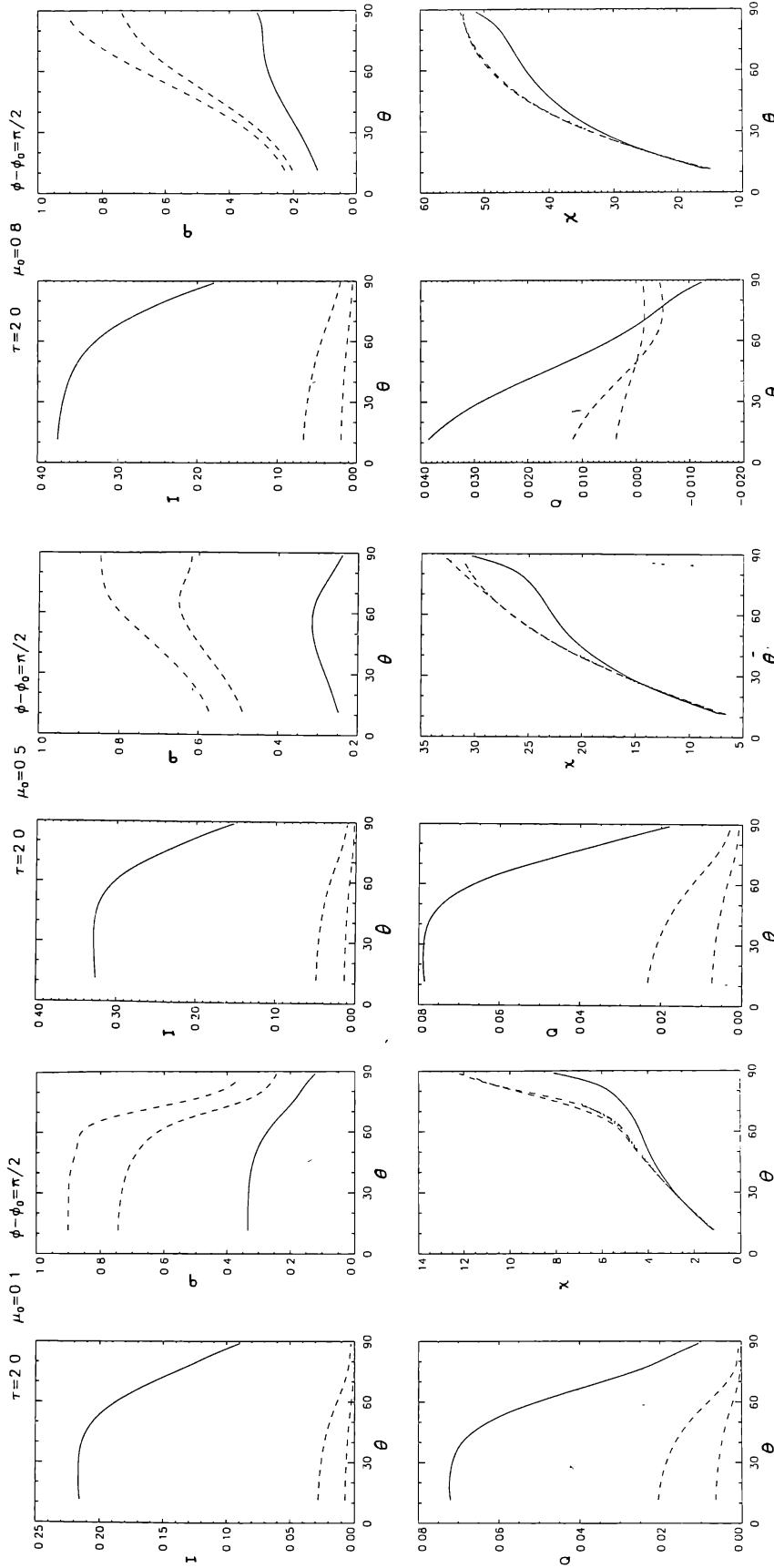


Figure 6(a). Same as figure 4(a) but for $\tau = 2.0$.

Figure 6(b). Same as figure 6(a) but for $\mu_0 = 0.5$.

Figure 6(c). Same as figure 6(a) but for $\mu_0 = 0.8$.

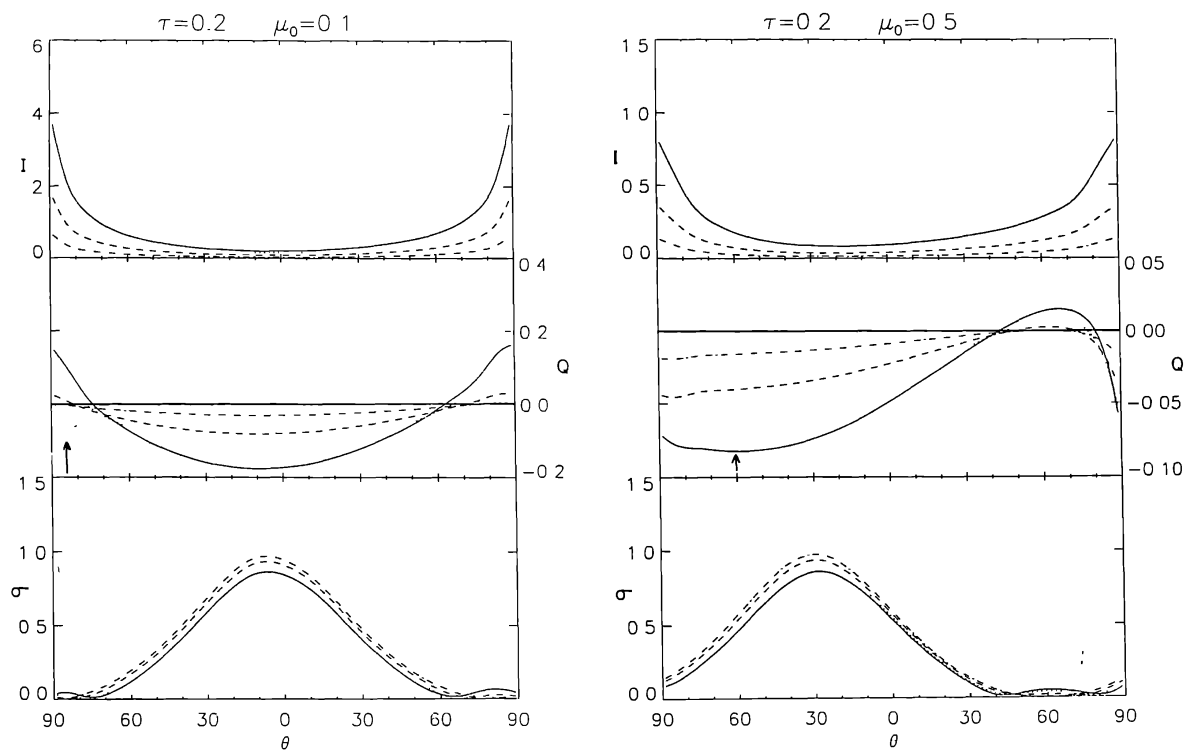


Figure 7(a). Same as figure 1(a) but for reflected light. Figure 7(b). Same as figure 7(a) but for $\mu_0 = 0.5$

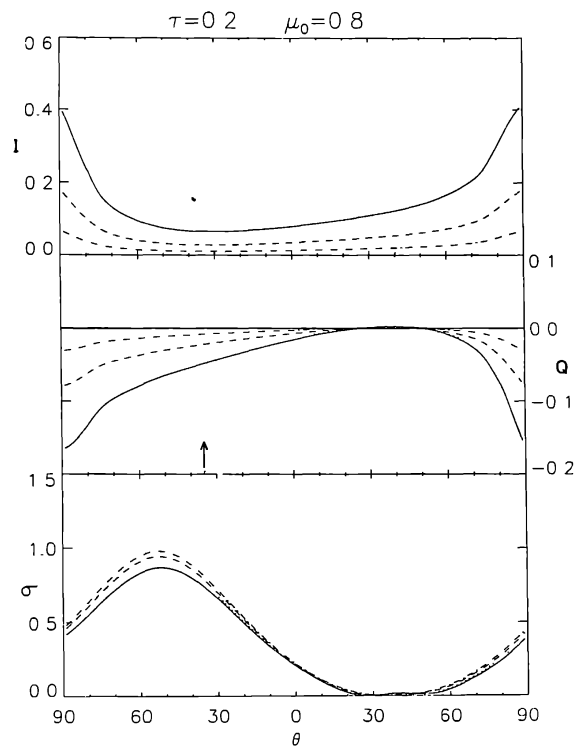


Figure 7(c). Same as figure 7(a) but for $\mu_0 = 0.8$.

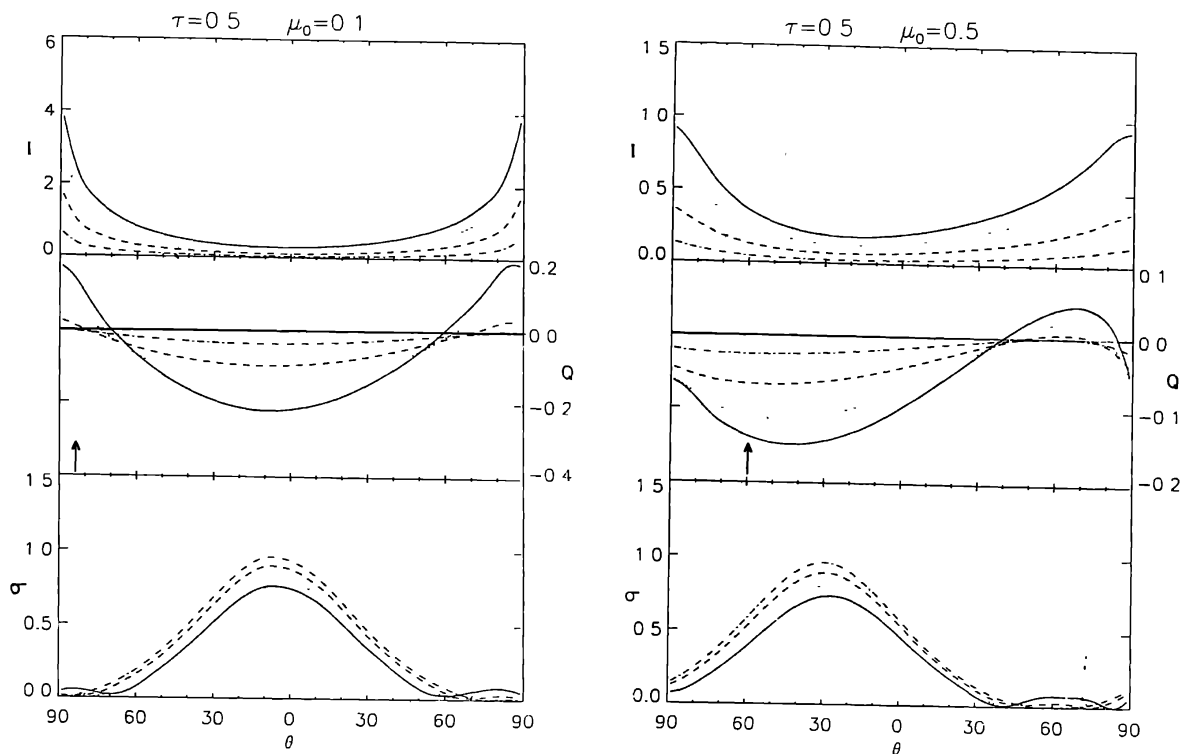


Figure 8(a). Same as figure 7(a) but for $\tau = 0.5$.

Figure 8(b). Same as figure 8(a) but for $\mu_0 = 0.5$

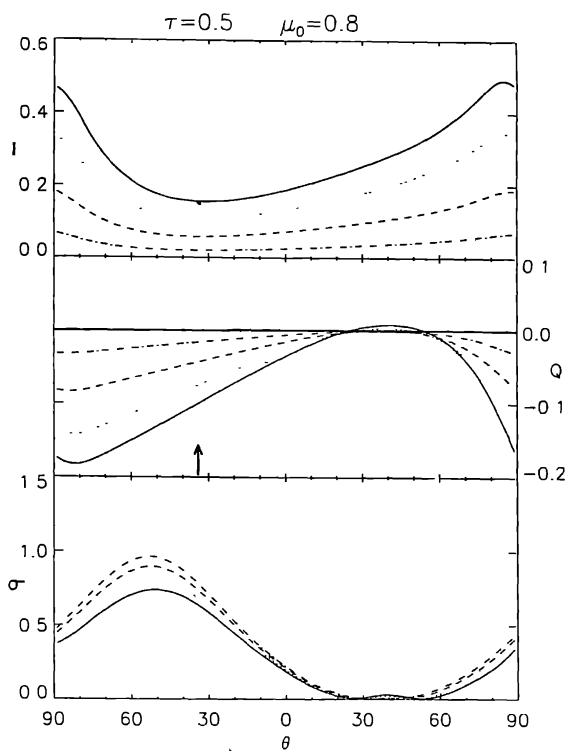


Figure 8(c). Same as figure 8(a) but for $\mu_0 = 0.8$.

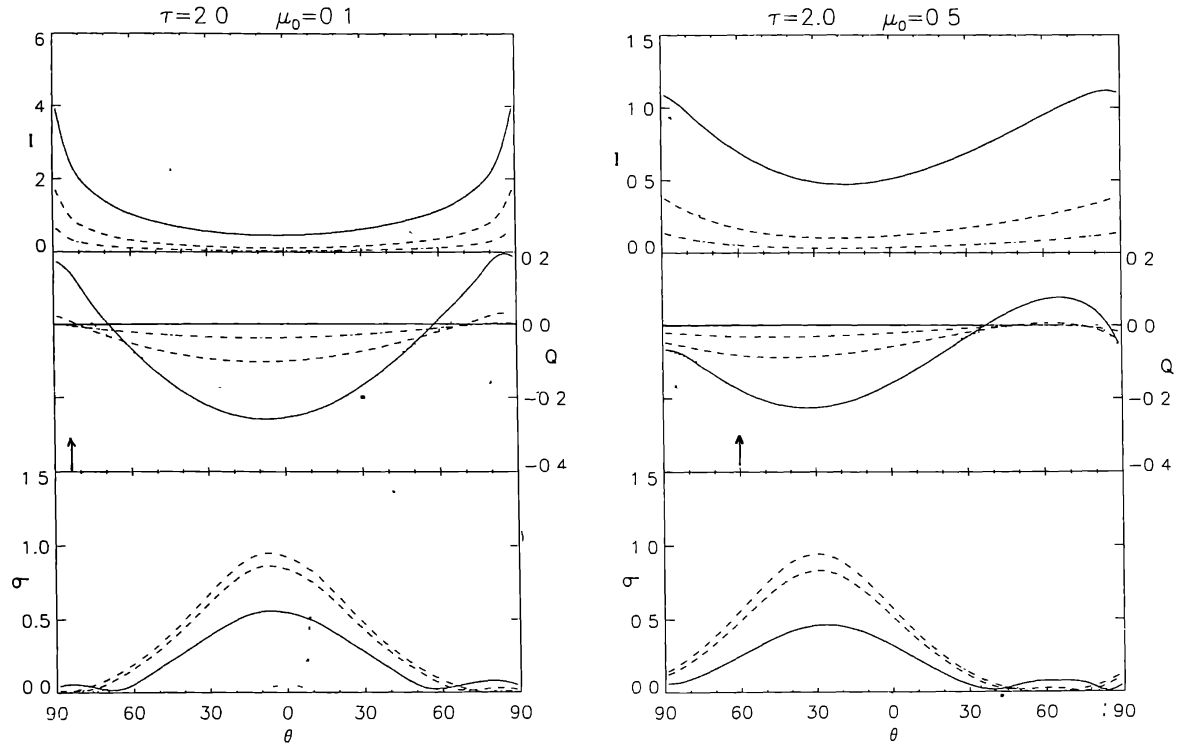


Figure 9(a). Same as figure 8(a) but for $\tau = 2.0$.

Figure 9(b). Same as figure 9(a) but for $\mu_0 = 0.5$.

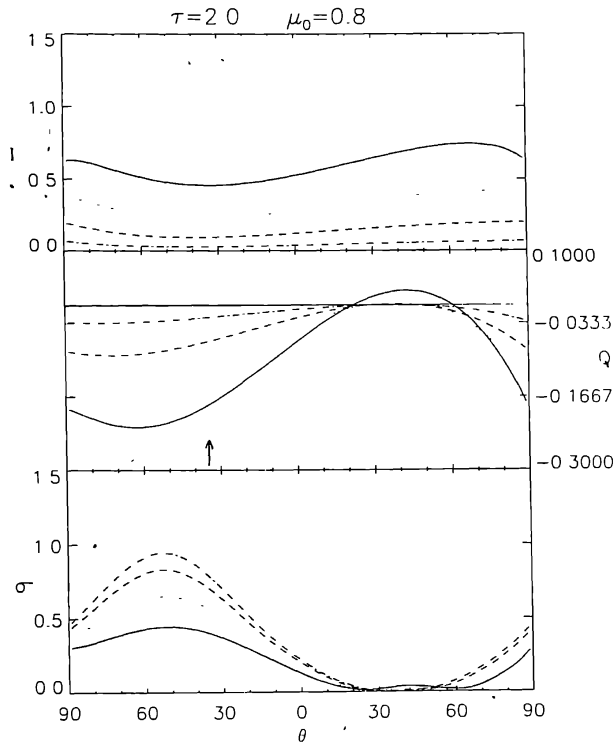


Figure 9(c). Same as figure 9(a) but for $\mu_0 = 0.8$.

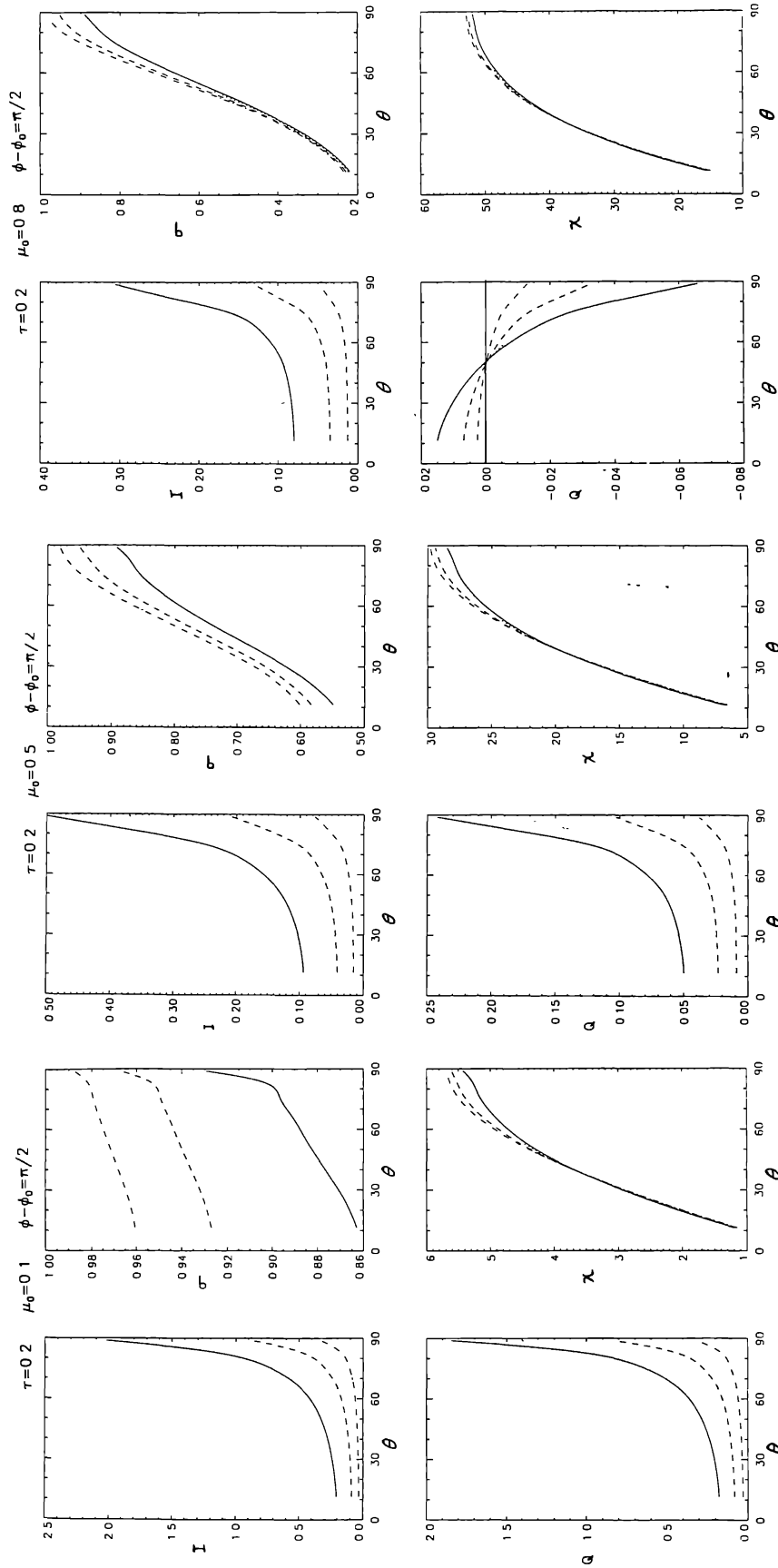


Figure 10(a). Top panels give total intensity (left) and Stokes Q parameter and χ in the reflected light at the azimuth angle $\phi - \phi_0 = \pi/2$ for $\tau = 0.2$ and $\mu_0 = 0.1$ (right) and the bottom panels show the Stokes Q parameter and χ in the reflected light at the azimuth angle $\phi - \phi_0 = \pi/2$ for $\tau = 0.2$ and $\mu_0 = 0.1$ (right). Same as figure 10(a) but for $\mu_0 = 0.5$. Figure 10(c). Same as figure 10(a) but for $\mu_0 = 0.8$.

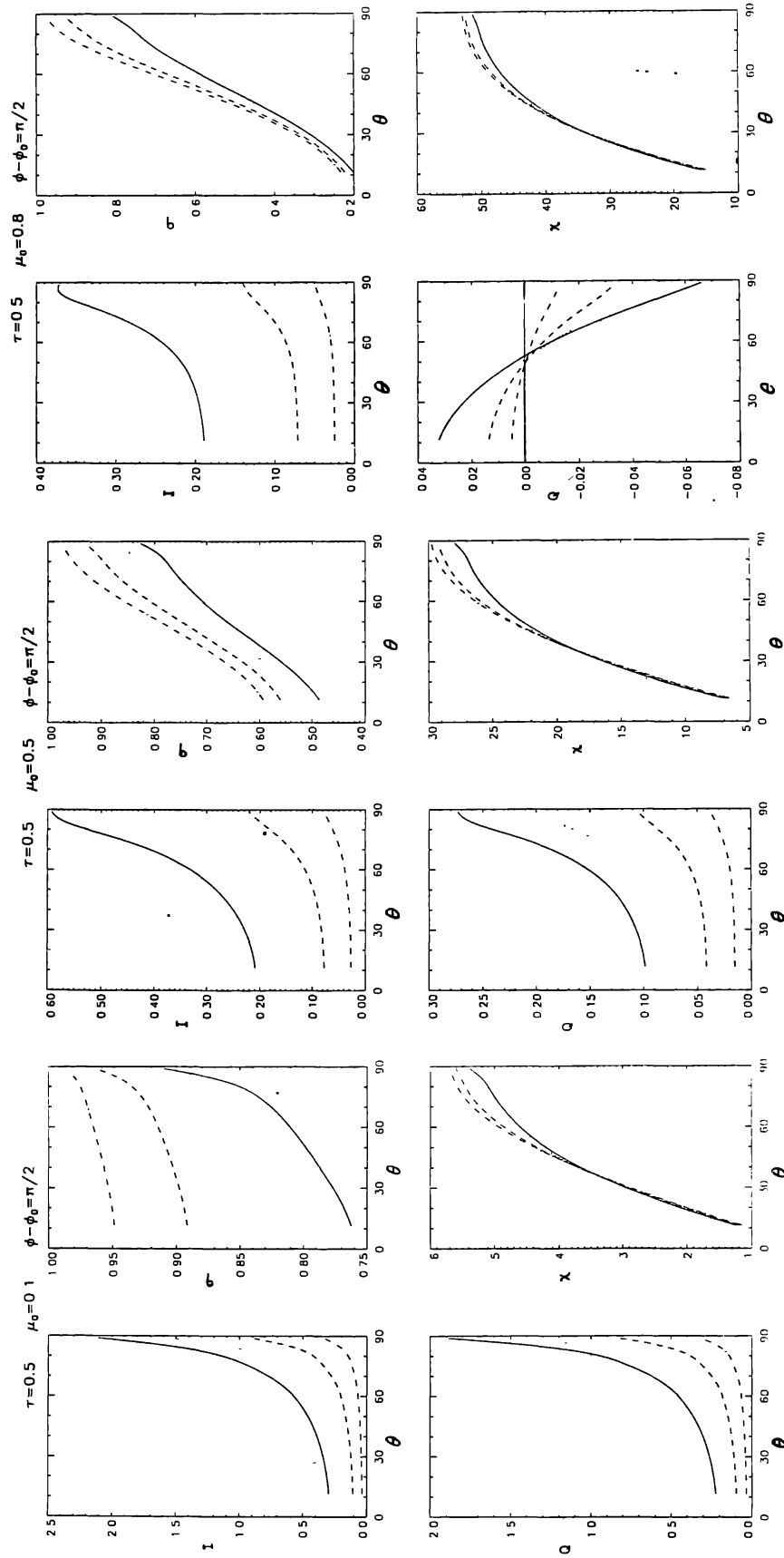


Figure 11(a). Same as figure 10(a) but for $\tau_0 = 0.5$. Figure 11(b). Same as figure 11(a) but for $\mu_0 = 0.5$. Figure 11(c). Same as figure 11(a) but for $\mu_0 = 0.8$.

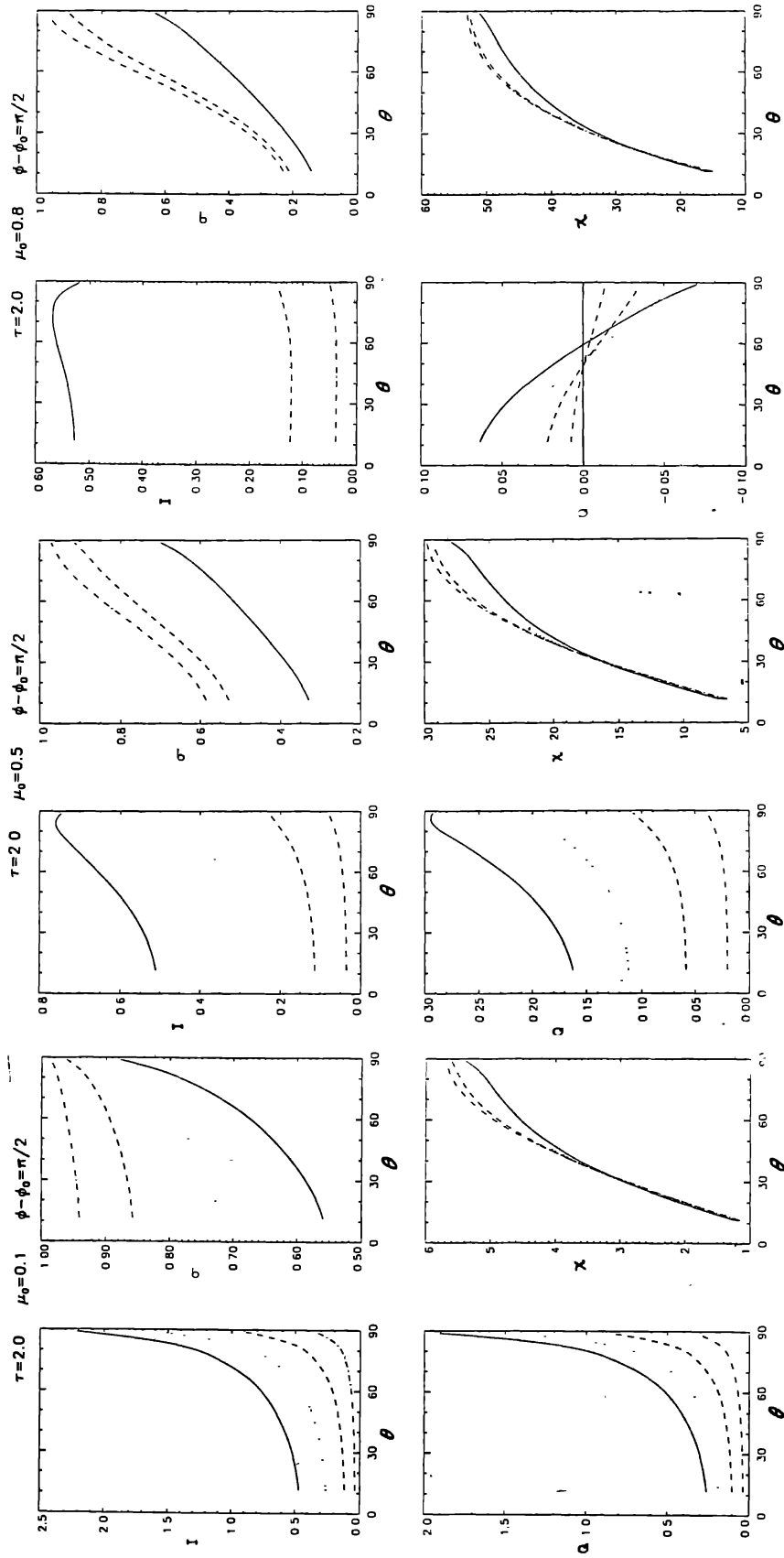


Figure 12(a). Same as figure 10(a) but for $\tau = 2.0$ Figure 12(b). Same as figure 12(a) but for $\mu_0 = 0.5$. Figure 12(c). Same as figure 12(a) but for $\mu_0 = 0.8$.

the sign). Whereas for a higher optical depth ($\tau = 2$), $I_r > I_l$ at all the angles of observation. For $\phi - \phi_0 = \pi/2$, and $\mu_0 = 0.1$, Q peaks at some particular angle for smaller optical thicknesses, but there is no such maximum found for $\tau = 2.0$.

Behaviour of neutral points

(i) When the sun is near the horizon, one finds only one neutral point (Babinet point) which is shifted away from the sun for higher ω 's and at smaller optical thickness. When the sun is between the horizon and the zenith ($\mu_0 = 0.5, 0.8$), two neutral points (Babinet and Brewster points) are generally seen in the sun's direction. Smaller ω 's have the tendency to bring the neutral points closer to the sun. To make this point clearer, the positions of the neutral points for different locations of the sun and for different optical thickness are tabulated in table 1. A value of $\omega \simeq 0.9$ may be able to explain the neutral point observations of Holzworth & Rao (1965). The same behaviour was seen for semi-infinite atmospheres by Abhyankar & Fymat (1970).

(ii) When $\phi - \phi_0 = \pi$, we find only one neutral point (Arago point) when the sun is near the horizon e.g. $\mu_0 = 0.1$. This neutral point moves towards the anti-solar point as ω decreases and disappears for very small ω , e.g. $\omega = 0.2$.

Table 1. Neutral points for the transmitted light The numbers in columns 3-7 are the zenith angles in degrees

Optical depth τ	Sun's position		$\omega = 1.0$ (conservative scattering)	$\omega = 0.8$	$\omega = 0.5$	$\omega = 0.2$	Remarks
	$\phi - \phi_0$	θ_0					
0.2	0	84°	62	65.2	70	75	Babinet
0.2	180 (anti solar direction)	84	72.5	76	80	86	Arago
0.2	0	60	43.47	45.4	48.6	52.7	Babinet
			80.5	77.5	73.5	68.0	Brewster
0.2	0	36	26.5	28	29.5	32.7	Babinet
			50.0	48.5	45.4	41.9	Brewster
0.5	0	84	56.5	61.4	67	74.2	Babinet
0.5	180	84	66.2	71	77.4	85.3	Two Arago
						87.6	points
0.5	0	60	39	42.1	47	51.7	Babinet
			86.9	82.2	75.8	68.6	Brewster
0.5	0	36	24	25.6	28	31.2	Babinet
			54.9	51.7	47	42.2	Brewster
2.0	0	60	36.7	44.6	54	—	Babinet
			82.1	70.2	60.6	—	Brewster
2.0	0	36	21.5	25.6	29.6	32.7	Babinet
			64.6	51.7	44.6	40.6	Brewster

Variation of σ

Here the notable result is that, σ , the amount of polarization increases with smaller ω 's for $I_l < I_r$ but decreases for $I_l > I_r$. This can be seen by comparing the figures for Q and σ . The amount of polarization attains maximum near 90° from the sun's position. When optical thickness is increased, the amount of polarization (σ) reduces. At $\phi - \phi_0 = 0$ and $\mu_0 = 0.5$ and 0.8 we get minima for σ at two positions in the sky. The angular separation between these positions increases as τ increases and for the same τ , the angular separation between the two minima increases as ω increases. The difference in σ for different ω 's at any angle θ increases as τ increases. At $\phi - \phi_0 = \pi$, the maximum of σ is shifted towards the horizon when the sun goes towards the zenith irrespective of τ and ω values.

Variation of χ

We have plotted χ for $\phi - \phi_0 = \pi/2$. Plane of polarization (χ) is found to be same for all albedos at the zenith, but it is different for different ω 's near the horizon and the differences increase for higher optical thickness. The plane of polarization is more inclined for $\tau = 2.0$ compared to the lesser optical thickness.

Reflected light

Qualitatively the reflected light behaves similar to the transmitted light when $\phi - \phi_0 = 0, \pi$ and $\pi/2$. It decreases monotonically with ω . As in the case of the transmitted light, the difference in polarization for different ω 's at any viewing angle θ increases as τ is increased.

If $\mu_0 \neq 0.1$, neutral points are seen in the anti-solar direction in the principal meridian for all optical thickness. For $\mu_0 = 0.1$, we get neutral points both in the solar and anti-solar directions. Neutral points are brought closer to the sun as optical thickness or ω decreases.

Discussion

Polarization studies considering model atmospheres (including ground reflection, aerosols and absorption by molecules) of the earth were done by Hitzfelder *et al.* (1976). They found that the position of the neutral points is insensitive to the ground reflection (surface albedo). It is however sensitive to the number of aerosol particles in the atmosphere. Our results are in conformity with their results and in addition clearly show that even the small particles which scatter according to non-conservative Rayleigh law can explain the shift in the observed positions of neutral points. Earlier works on this topic invoke non-Rayleigh type of scattering to account for the same phenomenon.

The present study shows the observed decrease in the negative area of polarization. But we find enhanced polarization in the other positive area when non-unitary albedos are used. This can be accounted if we include depolarization mechanisms like molecular anisotropy, reflection from the ground etc. The observations under polluted conditions show the presence of larger particles which select non-Rayleigh type of scattering laws.

We have applied our numerical code to study the polarization profiles of the molecular lines in the telluric bands, the results of which will be shortly reported.

Acknowledgments

The authors wish to thank Prof. A. Peraiah for his keen interest and encouragement during this project. We are indebted to Mr B. A. Varghese for his help in plotting the graphs. We gratefully acknowledge the useful suggestions of Prof. H. C. van de Hulst as the referee which helped us to improve the presentation of the paper.

References

- Abhyankar K. D., Fymat A. L., 1970, *A&A*, 4, 101.
Chandrasekhar S., 1960, *Radiative Transfer*, Oxford University Press, Dover
Coulson K. L., Dave J. V., Sekera Z., 1960, *Tables related to radiation emerging from a planetary atmosphere with Rayleigh scattering*, University of California Press, Berkeley & Los Angeles.
Coulson K. L., 1971, *JQSRT*, 11, 739.
Coulson K. L., Walraven R. L., Weigt G. I., Soohoo L. B., 1974, *Appl. Optics*, 13, 497.
Grant I. P., Hunt G. E., 1969, *Proc. Roy. Soc. London A.*, 313, 183.
Hitzfelder S. J., Plass G. N., Kattawar G. W., 1976, *Appl. Optics*, 15, 2489.
Holzworth G. C., Rao C. R. N., 1965, *Sci. Rept.*, AFCRL-65-167, Univ. of California, Los Angeles.
Kattawar G. W., Plass G. N., Hitzfelder S. J., 1976, *Appl. Optics*, 15, 632.
Peraiah A., 1978, *Kodaikanal Obs. Bull. Ser. A*, 2, 115.
Plass G. N., Kattawar G. W., Binstock J., 1973, *JQSRT*, 13, 1081.
Sekera Z. et al., 1955, *AF 19 (122)-239*, Univ. of California, Los Angeles.
Van de Hulst H. C., 1980, *Multiple Light Scattering*, Vols 1&2, Academic Press, New York.